An earthquake precursor- Outgoing Longwave Radiation (OLR) observed over the Indian and Indonesian regions during high-magnitude earthquakes (M≥ 6.0)

Pooja Sharma[1], Ananna Bardhan[1*], Raj kumari[2], and D. K. Sharma[1]
[1] Department of Sciences, Manav Rachna University, Faridabad-121004, Haryana, India
[2] Department of Physics, DAV Centenary College, Faridabad-121001, Haryana, India
[*]Corresponding author: ananna@mru.edu.in

ABSTRACT

The Earth prepares itself before an earthquake and during this time, several precursory signs have been seen across the ocean, land, and atmosphere. Earthquakes inflict significant harm to both human lives and property. Therefore, monitoring and understanding the strange behaviour of various geophysical parameters as precursors, have become extremely important. The Outgoing Longwave Radiations (OLR), emitted by the surface during the recent ten high-magnitude (M ≥6.0) earthquake (EQs) events, have been examined in the present work using the Data on OLR from the NCEP website. To analyse the OLR as precursory signatures of earthquakes, the climatological analysis for the seismic precursor identification (CAPRI) methodology was carried out. An apparent change in the OLR during 2 months before the earthquake events was observed. The maximum and minimum anomalies in OLR before all ten events were analysed. The maximum and minimum anomalous increase in OLR varied from 1.16 to 1.25 and 0.71 to 1.11 times greater during the earthquake years compared to historical time series respectively, during all the ten EQ events. The study indicates a strange shift in Outgoing Longwave Radiation during periods, influenced by the seismic activity. The extent of anomalies in OLR during earthquake events is maximum over the ocean than on the land. This is because the accumulation of water vapour traps the outgoing radiation, causing an elevation in temperature over the epicentre and Earthquake Preparation Zone (EPZ)

Keywords: - Earthquake precursor, Outgoing Longwave Radiation (OLR) anomaly, Earthquake Preparation Zone (EPZ), High magnitude earthquakes, Epicentre. India and Indonesia

INTRODUCTION

Earthquakes are highly destructive natural disasters that occur without warning, making prediction crucial for impact mitigation. Despite efforts, precise prediction remains challenging due to the complexity of seismic events. The various ground, atmospheric, and ionospheric precursors have been studied over the past few decades, offering insights into potential early warning signs. These precursors range from ground deformation (Pulinets and Boyarchuk, 2004), mechanical deformation (Niu, 2008), gas emissions (Pulinets et al., 2003), electromagnetic precursors (Uyeda et al., 2009), changes in ionospheric parameters (Liu et al., 2004), and thermal anomaly (Pulinets et al., 2006; Zhang et al., 2013; Bardhan et al., 2022; Ghosh et al., 2024; Sharma et al., 2024; Qasim et al., 2024).

This work examines thermal precursors, which are temperature anomalies in the Earth's crust or near-surface environment that occur before seismic activities. Thermal anomalies have been detected in areas of earthquake preparation zones, several days prior to the seismic events (Tronin et al., 2002; Tramutoli et al., 2005) and are often attributed to thermal flux emanating from the Earth's crust in seismically active regions (Ouzounov and Freund, 2004). Several investigations about the occurrence of pre-earthquake thermal anomalies in locations like India, Japan, China, Sumatra, Italy, Iran, and Haiti, have been studied by several researchers (Tronin et al., 2002; Ouzounov and Freund, 2004; Tramutoli et al., 2005; Choudhury et al., 2006).

Schulz et al. (1997) observed latent heat anomalies associated with earthquakes, using remote sensing satellite data. In various regions of the world, efforts have been initiated to utilise thermally associated satellite observations to identify anomalous indicators connected to earthquakes, which include infrared/microwave brightness temperature (Jing et al., 2018), surface temperature (Tronin et al., 2002), air temperature (Weiyu et al., 2018), OLR (Ouzounov et al., 2007), and Surface Latent Heat Flux (SLHF) (Bardhan et al., 2022; Sharma et al., 2024). In the epicentral zones and along the faults, these anomalous thermal signals were observed for two months before significant earthquakes (Pulinets et al., 2006).

A key parameter used to describe Earth's radiation environment is the measurement of Outgoing Longwave Radiation (OLR) (Liebmann and Smith, 1996). The Earth's surface absorbs solar energy in the form of shortwave (SW) radiation. Due to the surface's low thermal conductivity, the absorbed heat doesn't penetrate deeply. Instead, it is mostly re-emitted at night as long wavelength radiation (LWR) energy. OLR which is associated with the top of the atmosphere, integrates emissions from the ground, lower atmosphere, and clouds and is primarily used for studying Earth's radiative budget and climate dynamics (Gruber and Krueger, 1984).

Several research studies have been performed related to OLR (Ouzounov et al., 2007; Rawat et al., 2011; Fu et al., 2020). Studies have revealed that abnormal thermal patterns, identified through OLR or thermal infrared radiation (TIR), frequently emerge prior to or during the earthquake preparation phase (Tramutoli et al., 2005; Pulinets et al., 2006). Rawat et al. (2011) studied earthquakes in the Indian and Italy regions and found 30-45 Wm^{-2} more energy than the normal period at the Earth's surface. Shah et al. (2019) reported significant OLR anomalies up to 21 days before major earthquakes in Pakistan and Iran, with flux variations exceeding +2σ occurring 3 to 30 days prior. Daily OLR data have also been used to examine the variability within earthquake-prone zones (Ouzounov et al., 2007). Fu et al. (2020) identified OLR anomaly as a potential earthquake precursor, with thermal releases near the epicentre observed 2–15 days before significant events. Hameed et al. (2024) identified several atmospheric precursors potentially linked to seismic events, including variations in latent heat flux, and OLR, occurring 5–10 days before the earthquake. Tronin (2006) detected anomalies 4–20 days before a major earthquake, while Hafeez et al. (2022) identified them within a 5–10 day window. Similarly, Qasim et al. (2024) also analyzed the March 31, 2020, Mw 6.5 Idaho earthquake using high-resolution satellite data over a 45-day period. Numerous studies, including Akhoondzadeh (2024), who have reported abnormal physical and chemical precursors 1–30 days before significant seismic events. In the present work, the precursory analysis of the thermal parameter - Outgoing Longwave Radiation (OLR), is attempted on ten high-magnitude earthquakes (M≥6.0) over the Indian and Indonesian regions.

DATA AND METHODOLOGY

The Outgoing Longwave Radiation (OLR) data during the ten recent earthquakes were collected from the National Centre for Environmental Prediction/National Centre for Atmospheric Research (NCEP-NCAR) site. The data collected spanned over the Earthquake Preparation Zone (EPZ), including the epicentres of the considered earthquake events. The daily OLR data has been taken from the link: https://iridl.ldeo.columbia.edu/SOURCES/.NOAA/.NCEP/.CPC/.CBO_V1/.r0p25/.MON/.NRT/.anom. These data sets are built by integrating data from satellites with measured values from various sites throughout the world. A worldwide dataset of various climatological and surface variables is maintained by NCEP. The fluxes considered in functional meteorological forecasting techniques contain in-situ data. The NCEP-NCAR (National Centers for Environmental Prediction/National Center for Atmospheric Research) integrates the data from remote sensing, aircraft, pibal, rawinsonde, ship, ground instruments etc, thus, provides assimilated global reanalysis data with an accuracy limit of 10-30 W/m^2 (Zhang et al., 2013). The daily OLR values have a spatial resolution of 1.87×1.90 degrees across the globe from 1 Jan 1948 to the current time respectively. The earthquake details presented in Table 1 are sourced from the United States Geological Survey (USGS) (http://earthquake.usgs.gov/activity/world.html) website. This table includes information on event locations, dates, times, epicentre coordinates, and focal depths for earthquakes in Pariaman, Biak, Papua, Gorontalo, Assam, Port Blair, Ternate, Bengkulu and Luwuk.

DATA SELECTION AND ANALYSIS FOR OUTGOING LONGWAVE RADIATION

To investigate the anomalies observed in OLR before all ten earthquakes, the statistical method - Climatological Analysis for Seismic Precursor Identification (CAPRI) are applied. This section provides a concise overview of the mathematical algorithm employed by the CAPRI method. For a more comprehensive understanding, readers can refer to the detailed discussions in Piscini et al. (2017, 2019). Dobrovolsky et al. (1979) proposed an observable association between the expected circular area of mechanical, thermal, and electromagnetic activity prior to them and the estimated magnitude of the upcoming earthquake. Since seismic precursors typically form across vast regions surrounding impending faults, $r = 10^{0.43M}$. where M is the anticipated earthquake's magnitude and r is the “strain radius,” which is the affected area's radius in kilometres. The earthquake preparation zone (EPZ) is determined using $r = 10^{0.43M}$. Over the EPZ, outgoing longwave radiation anomalies have been investigated.

The Climatological Analysis for Seismic Precursor Identification (CAPRI) method is employed to identify anomalies in climatological variable time series through statistical analysis. In this study, the focus is on the OLR parameter. Before analysis, the data is spatially averaged over the epicentral region. OLR(d)y denotes the average OLR value for a specific day 'd' (equivalent to 2 months or 60 days) in a given year ‘y’ (spanning a dataset of 38 years). The CAPRI methodology is designed to remove long-term trends that may exist in the day-to-day dataset. Its methodology is primarily proposed to minimize probable "global warming".

To effectively eliminate these trends, as detailed in studies by Piscini et al. (2017, 2019), a 38-year dataset is analyzed by considering individual time sequences corresponding to the same day. For each day of the year across the entire time span, a linear regression analysis is performed on the variables under examination. The slope of this fit, denoted as m (d) that representing the OLR variation on the same day ‘d’ for each year, is then utilized to remove the long-term variations in the variable. A linear fit is a good trend given the short time span analysed (about 40 years) in relation to climate change (Brohan et al., 2006).

In this process, the initial year in the time-series data, denoted as y_o, serves as a "reference point." The growth or change in the variable is determined by multiplying the slope obtained from the linear fit by the number of successive years following the first year. This correction is applied to eliminate the long-term trends for the subsequent years in the dataset.

$$OLR'(d)_y = OLR(d)_y - m(d) \times (y - y_o) \quad ---- \quad (1)$$

This method is carried out for each of the days being considered. The advantage of performing a new fit for each day lies in its ability to account for the potential influence of localized seasonal variations over time, as discussed in Piscini et al. (2017, 2019). For each year under examination, the resulting data consists of daily spatially averaged Outgoing Longwave Radiation (OLR) values, organized day by day. It's important to note that, irrespective of the fact that the year did not conform to the estimates of the consistent pattern, any detected pattern was also removed from that specific year. Subsequently, the variables from the time-series data are aggregated across all years, focusing on each day 'd'. This aggregation provides the historical mean, denoted as $OLR_h(d)$ (where 'h' signifies the historical time series), spanning the previous 37 years, as the year of the earthquake series is excluded from this calculation:

$$OLR_h(d) = \frac{1}{N_y} \sum_{y=\alpha}^{\beta} OLR'(d)_y \quad ---- \quad (2)$$

Here, N_y represents the total number of years that have been aggregated, where α is the initial year and β is the 37th year. In this context, the program also calculates the standard deviation (σ) for each day. The behaviour factor of the subsequent year, denoted as 'ỹ,' is subsequently compared to the historical series as described in Eq. (1). To facilitate this comparison, we set the overall average in the studied period to correspond with the average of the historical time series to make this comparison possible:

$$OLR(d)_{\tilde{y}} = OLR'(d)_{\tilde{y}} - [(OLR'_{\tilde{y}})_d - (OLR_h)_d] \quad ---- \quad (3)$$

In the current study, it's important to account for the possibility of a single year deviating significantly from the historical average, which could potentially introduce false results. Therefore, the equation mentioned above is employed to effectively filter out these short-term anomalies. Specifically, in this study, anomalous days are identified as those where the variable's values deviate by at least 2σ above or below the historical average.

RESULTS

In this study, we have examined ten recent high-magnitude ($M \geq 6.0$) earthquakes that occurred between years 2015 and 2022. In all these events, the behaviour of OLR as a precursor of earthquakes has been analysed. The details of all the earthquake events are taken from the website of the National Earthquake Information Centre (NEIC), and United States Geological Survey (USGS), which includes location, date and time, epicentre, magnitude, and focal depth (Table 1).

Variation of OLR during the earthquake events

1. Pariaman (Indonesia)

This earthquake occurred in Pariaman, Indonesia (Epicentre: 1.14° S and 98.65° E) on September 10, 2022, and had a magnitude of 6.0 and a focal depth of 20.0 km. The variation in OLR has been analysed for the purpose of identifying precursory signatures during the earthquake event. (Figure 1) shows a comparison of the time series year 2022 (earthquake year) with the historical time series years 1985-2021 of OLR. In (Figure 1),the black curve with a cross and the red curve with a triangle denotes the earthquake year and a historical time series of 37 years, respectively. The coloured curve represents 2.0 (blue) standard deviations from the mean historical time series, respectively. In analysis, we examined OLR values for 59 days leading up to an earthquake event, with the 60th day representing the day of the earthquake (purple line). We have considered the variation of OLR as an anomaly only when its value is above 2 standard deviations from the historical time series. (Figure 1**)** reveals numerous instances where the OLR exceeds the values found in the historical time series.

Table1. Details of the studied earthquakes and their magnitude and focal depth

Sr. No.	Location	Date and time (UTC)	Epicentre (Geog. Lat., Geog. Long.)	Magnitude	Focal depth (km)
1	Pariaman, Indonesia	10.09.2022 (23:10:43)	1.14° S, 98.65° E	6.0	20
2	Biak, Indonesia	10.09.2022 (00:05:12)	2.23° S, 138.17° E	6.2	21
3	Papua, Indonesia	09.09.2022 (23:31:47)	2.24° S, 138.19° E	6.2	18
4	Pariaman, Indonesia	13.03.2022 (21:09:22)	0.62° S, 98.62° E	6.7	28
5	Gorontalo, Indonesia	06.11.2021 (14:37:36)	0.04° S, 124.28° E	6.0	34
6	Dhekiajuli, Assam, India	28.04.2021 (02:21:26)	26.78° N, 92.45° E	6.0	34
7	Port Blair, India	17.07.2020 (14:03:40)	11.84° N, 94.93° E	6.1	10
8	Ternate, Indonesia	14.11.2019 (21:12:54)	1.53° N,126.41° E	6.0	23
9	Bengkulu, Indonesia	13.08.2017 (03:08:10)	3.76° S, 101.62° E	6.4	31
10	Luwuk, Indonesia	15.03.2015 (23:17:16)	0.54° S, 122.30° E	6.1	31

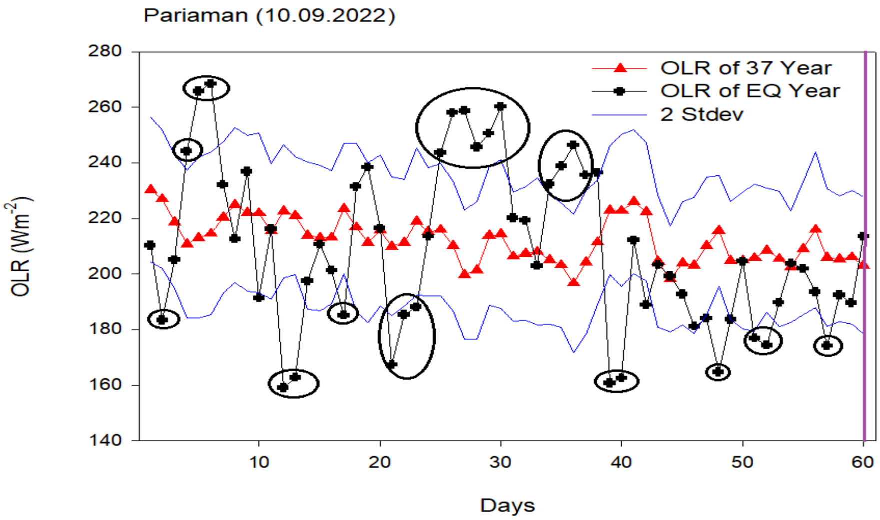

Figure 1. Daily variation of outgoing longwave radiation during the earthquake year (black cross) - 2022 vs. mean historical time series 1985-2021 (red triangle) during the earthquake events that occurred in Pariaman, Indonesia (10.09.2022) having epicentre (1.14° S, 98.65° E). The blue coloured curve indicates 2.0 standard deviation from the mean - historical time series. The purple line shows earthquake day.

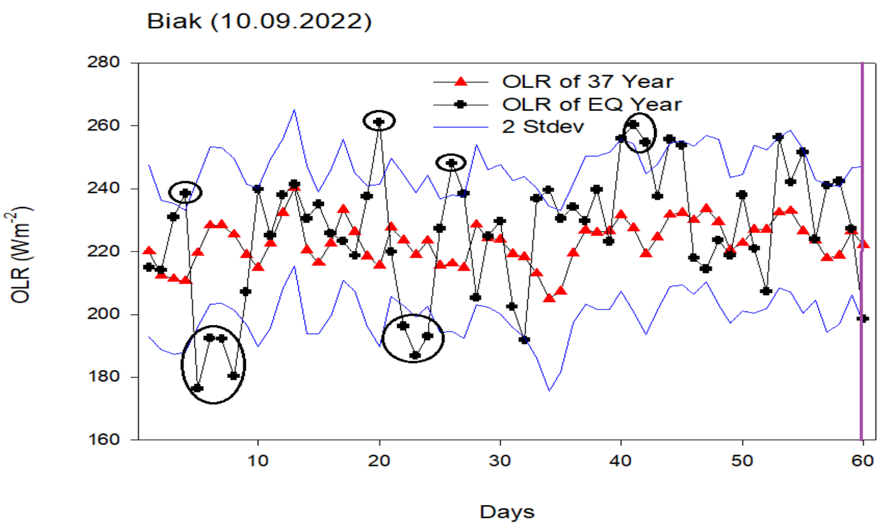

Figure 2. Daily variation of outgoing longwave radiation during the earthquake year (black cross) - 2022 vs. mean historical time series 1985-2021 (red triangle) during the earthquake events that occurred in Biak, Indonesia (10.09.2022) having epicentre (2.23° S, 138.17° E). The blue coloured curve indicates a 2.0 standard deviation from the mean - historical time series. The purple line shows earthquake day.

During the earthquake year, there is an increase in the OLR on the 2nd, 12th -13th, 17th, 39th -40th, 48th, 51st -52nd and 57th, days with the values 183.37 Wm^{-2}, 160.91 Wm^{-2}, 185.12 Wm^{-2}, 161.65 Wm^{-2}, 164.69 Wm^{-2}, 175.64 Wm^{-2}, and 174.14 Wm^{-2}, respectively, greater than 2σ from the mean historical time series. Again, it was observed that OLR values exhibited an increase during several periods: from the 4th to the 6th days, the 21st to the 23rd day, the 25th to the 30th days, and from the 34th to the 37th days with the average OLR values during the earthquake year and historical time series were ∽259.40 Wm^{-2}, ∽180.26 Wm^{-2}, ∽252.76 Wm^{-2}, ∽238.23 Wm^{-2}, and ∽212.77 Wm^{-2}, ∽213.33 Wm^{-2}, ∽210.73 Wm^{-2}, ∽202.29 Wm^{-2}, respectively. The analysis distinctly shows that the maximum OLR anomalies, serving as precursory signatures, occur in the period leading up to the earthquake day.

2. Biak (Indonesia)

The earthquake that occurred on September 10, 2022, had a magnitude of 6.2 and a focal depth of 21.0 km (epicentre 2.23° S and 138.17° E) in Biak, Indonesia. (Figure 2**)** shows a comparison of the time series year 2022 (earthquake year) with the historical time series years 1985–2021 of OLR. The 37-year historical time series and the earthquake year are indicated in (Figure 2) by the red curve with a triangle and the black curve with a cross, respectively. (Figure 2) shows many instances in which the OLR exceeds the historical time series. There is an increase in the OLR on the 4th, 20th, 26th, 41st – 42nd, and 44th days with a value ~238.45 Wm^{-2}, ~261.17 Wm^{-2}, ~248.03 Wm^{-2}, ~257.91 Wm^{-2}, and ~255.67 Wm^{-2}, respectively, of greater than 2σ from the mean historical time series. Again, it was found that the OLR values increased from the 5th to 8th days, and from the 22nd to 24th days, with the average OLR values during the earthquake year and historical time series being ~185.33 Wm^{-2}, ~192.03 Wm^{-2} and ~225.42 Wm^{-2}, ~222.02 Wm^{-2} respectively. Several days show the anomalous behaviour of OLR during the pre-earthquake period. It is clear that from (Figure 2**)** before the earthquake day, the highest numbers of anomalies in OLR as precursory signatures are observed.

3. Papua (Indonesia)

The next earthquake event occurred on September 09, 2022, with a magnitude of 6.2 (epicentre: 2.24° S, 138.19° E) and a focal depth of 18.0 km in Papua, Indonesia. (Figure 3) shows a comparison of the time series year 2022 (earthquake year) with the historical time series years 1985–2021 of OLR. (Figure 3) shows many instances in which the OLR exceeds the 2σ from the mean historical time series. On several days, the increase in the OLR values on the 5th, 21st, 27th, 35th, 42nd - 43rd and 45th days with values ~238.45 Wm^{-2}, ~261.17 Wm^{-2}, ~248.03 Wm^{-2}, ~239.58 Wm^{-2}, ~257.55 Wm^{-2} and ~255.67 Wm^{-2}, respectively, greater than 2σ from the mean historical time series. Again, it was found that the OLR values rise from the 6th to 9th days, and from the 23rd to 25th days, with the average OLR values during the earthquake year and historical time series being ~185.33 Wm^{-2}, ~192.03 Wm^{-2} and ~225.44 Wm^{-2}, ~222.02 Wm^{-2} respectively. Several days show the anomalous behaviour of OLR during the pre-earthquake period. It is clearly observed that the maximum anomalies in OLR as precursory signatures are mostly observed before the earthquake day.

4. Pariaman (Indonesia)

The earthquake that occurred on March 13, 2022, had a magnitude of 6.7 and a focal depth of 28.0 km (epicentre: 0.62° S and 98.62° E) in Pariaman, Indonesia. (Figure 4) shows a comparison of the time series year 2022 (earthquake year) with the historical time series years 1985–2021 of OLR. The 37-year historical time series and the earthquake year are indicated in (Figure 4) by the red line with a triangle and the black line with a cross, respectively. (Figure 4) shows many instances in which the OLR exceeds the historical time series. There is an increase in the OLR on the 14th, 16th, 28th to 29th, 52nd to 53rd and 56th days with values ~231.66 Wm^{-2}, ~245.65 Wm^{-2}, ~167.31 Wm^{-2}, ~190.51 Wm^{-2}, and ~197.21 Wm^{-2}, respectively, greater than 2σ from the mean historical time series. Again, it was found that the OLR values rise from the 1st to 4th days, 8th to 10th days, and from the 23rd to 25th days, with the average OLR values during the earthquake year and historical time series being ~240.07 Wm^{-2}, ~233.46 Wm^{-2}, ~179.13 Wm^{-2}, and ~205.54 Wm^{-2}, ~195.6 Wm^{-2}, ~222.11 Wm^{-2} respectively. It is clear that from (Figure 4) several days before the earthquake day, the highest numbers of anomalies in OLR as precursory signatures are observed.

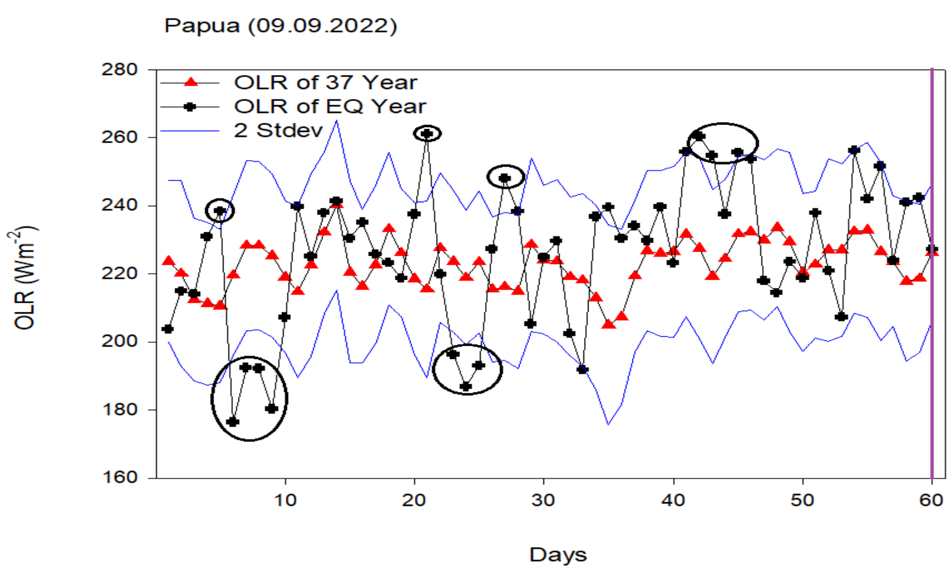

Figure 3. Daily variation of outgoing longwave radiation during the earthquake year (black cross) - 2022 vs. mean historical time series 1985-2021 (red triangle) during the earthquake events that occurred in Papua, Indonesia (09.09.2022) having epicentre (2.24° S, 138.19° E). Blue coloured curve indicates 2.0 standard deviation from the mean - historical time series. The purple line shows earthquake day.

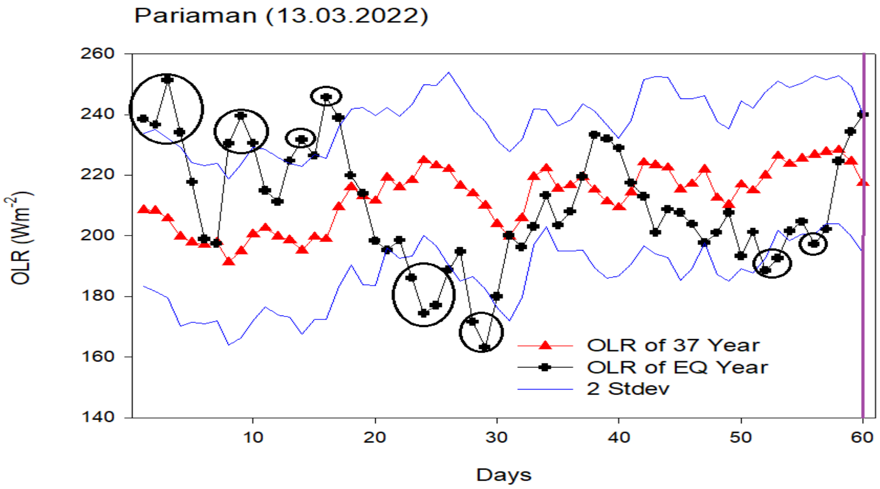

Figure 4. Daily variation of outgoing longwave radiation during the earthquake year (black cross) - 2022 vs. mean historical time series 1985-2021 (red triangle) during the earthquake events that occurred in Pariaman, Indonesia (13.03.2022) having epicentre (0.62° S, 98.62° E). Blue coloured curve indicates 2.0 standard deviation from the mean - historical time series. The purple line shows earthquake day.

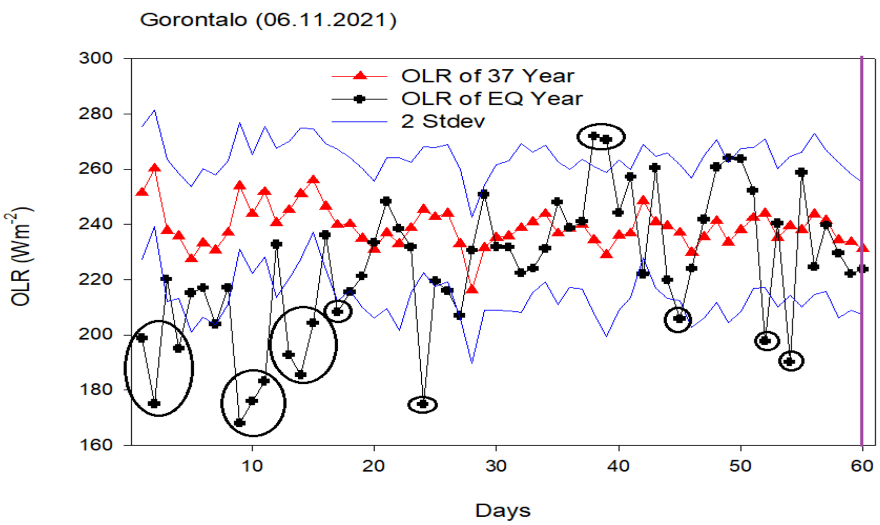

Figure 5. Daily variation of outgoing longwave radiation during the earthquake year (black cross) - 2021 vs. mean historical time series 1984-2020 (red triangle) during the earthquake events that occurred in Gorontalo, Indonesia (06.11.2021) having epicentre (0.04° S, 124.28° E). Blue coloured curve indicates 2.0 standard deviation from the mean - historical time series. The purple line shows earthquake day.

5. Gorontalo (Indonesia)

The next earthquake event occurred on Nov 6, 2021, with a magnitude of 6.0 (epicentre 0.04° S, 124.28° E) and a focal depth of 34.0 km in Gorontalo, Indonesia. (Figure 5) shows a comparison of the time series 2021 (earthquake year) with the historical time series 1984–2020 of OLR. (Figure 5 shows many instances in which the OLR exceeds the 2σ from the mean historical time series. From (Figure 5), one can observe many instances where the OLR is higher than the historical time series. There is an increase in the OLR on the 1st- 2nd, 4th, 17th, 24th, 38th -39th, 45th, 52nd and 54th, days with values ~186.93 Wm^{-2}, ~195.02 Wm^{-2}, ~208.26 Wm^{-2}, ~174.87 Wm^{-2}, ~271.31 Wm^{-2} , ~205.81 Wm^{-2}, ~197.75 Wm^{-2} and ~190.17 Wm^{-2}, respectively, of greater than 2σ from the mean historical time series. It was found that the OLR values rise from the 9th to 11th days, and from the 13th to 15th days, with the average OLR values during the earthquake year and historical time series being ~175.74 Wm^{-2}, ~194.16 Wm^{-2}, and ~249.83 Wm^{-2}, ~250.80 Wm^{-2} respectively. It is clearly observed that the maximum number of anomalies in OLR as precursory signatures are present before the earthquake day.

6. Dhekiajuli (Assam)

The next earthquake considered was Dhekiajuli, Assam (India), that occurred on April 28, 2021, with a magnitude of 6.0 having epicentre: 26.78° N, 92.45° E and focal depth, 34.0 km. (Figure 6) shows a comparison of the time series 2021 (earthquake year) with the historical time series years 1984–2020 of OLR. From this figure, one can observe many instances where the OLR is higher than the historical time series. The variation in the OLR on 38th-39th,42nd, 44th, 46th, 48th, and 52nd days with values ~259.95 Wm^{-2}, ~250.22 Wm^{-2}, ~256.29 Wm^{-2}, ~258.49 Wm^{-2}, ~212.28 Wm^{-2}, and ~260.25 Wm^{-2}, respectively, greater than 2σ from the mean historical time series. Again, it was found that the OLR values rise from the 1st to 4th, 10th to 14th, 16th to 19th, 23rd to 28th, 33rd to 35th, and 55th to 60th days, with the average OLR values during the earthquake year and historical time series being ~257.64 Wm^{-2}, ~254.84 Wm^{-2}, ~262.72 Wm^{-2}, ~261.35 Wm^{-2}, ~254.71 Wm^{-2}, ~258.22 Wm^{-2} and ~237.09 Wm^{-2}, ~230.11 Wm^{-2}, ~240.92 Wm^{-2}, ~225.98 Wm^{-2}, ~233.82 Wm^{-2}, ~218.35 Wm^{-2}, respectively.

7. Port Blair (India)

The earthquake occurred on July 17, 2020, having magnitude 6.1, epicentre 11.84° N, 94.93° E and focal depth 10.0 km in Port Blair, India. (Figure 7) shows a comparison of the time series 2020 (earthquake year) with the historical time series years 1983–2019 of OLR. In Figure 7, the black curve with a cross and the red curve with a triangle denote the earthquake year and a historical time series of 37 years, respectively. Initially, OLR is greater than 2σ on the 24th, 37th, 55th-56th, and 60th days with values ~215.03 Wm^{-2}, ~242.89 Wm^{-2}, ~145.09 Wm^{-2}, and ~222.04 Wm^{-2}, respectively, from the mean historical time series. Several times during the two months preceding the earthquake, the OLR was greater than two standard deviations. However, the frequency of the aforementioned events is greatest on 14th-16th, and 28th to 30th day, with the average OLR values during the earthquake year and historical time series of ~220.86 Wm^{-2}, ~166.89 Wm^{-2} and ~191.83 Wm^{-2}, ~203.63 Wm^{-2}, respectively. It is clear to see that days from the earthquake day, the highest numbers of anomalies in OLR as observed precursory signatures

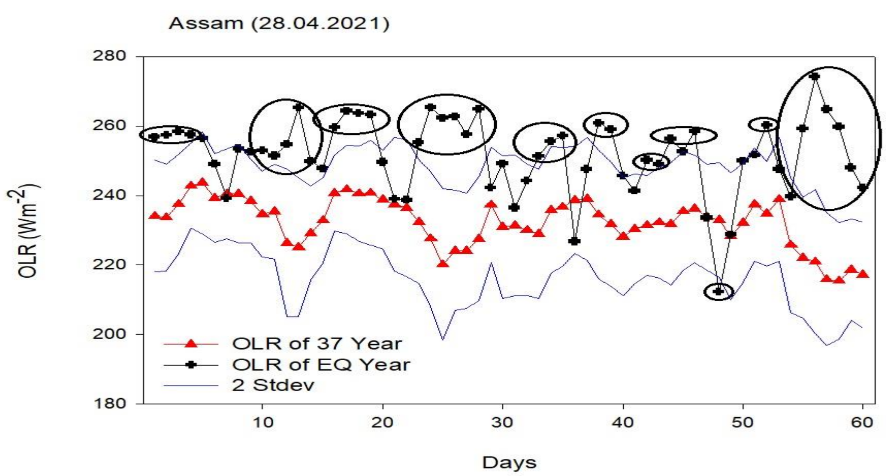

Figure 6. Daily variation of outgoing longwave radiation during the earthquake year (black cross) - 2021 vs. mean historical time series 1984-2020 (red triangle) during the earthquake events that occurred in Dhekiajuli, Assam, India (28.04.2021) having epicentre (26.78° N, 92.45° E). Blue coloured curve indicates 2.0 (blue) standard deviation from the mean - historical time series. The purple line shows earthquake day.

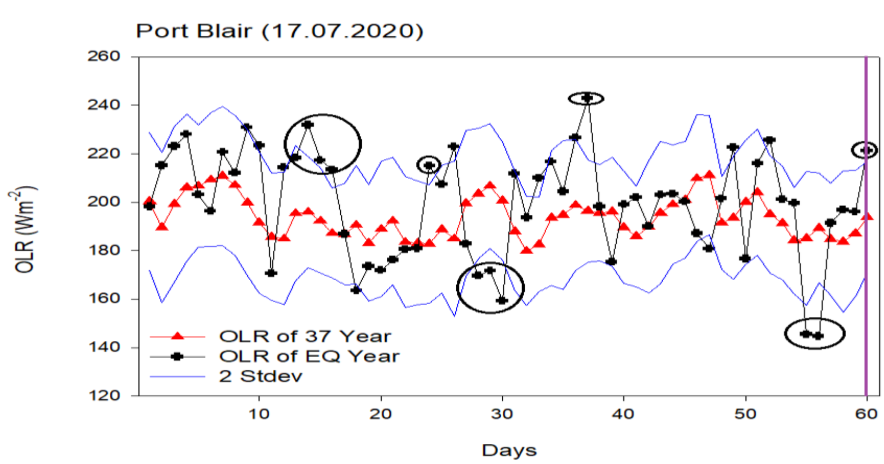

Figure 7. Daily variation of outgoing longwave radiation during the earthquake year (black cross) - 2020 vs. mean historical time series 1983-2019 (red triangle) during the earthquake events that occurred in Port Blair, India (17.07.2020), having epicentre 11.84° N, 94.93° E. Blue coloured curve indicates 2.0 standard deviation from the mean - historical time series. The purple line shows earthquake day.

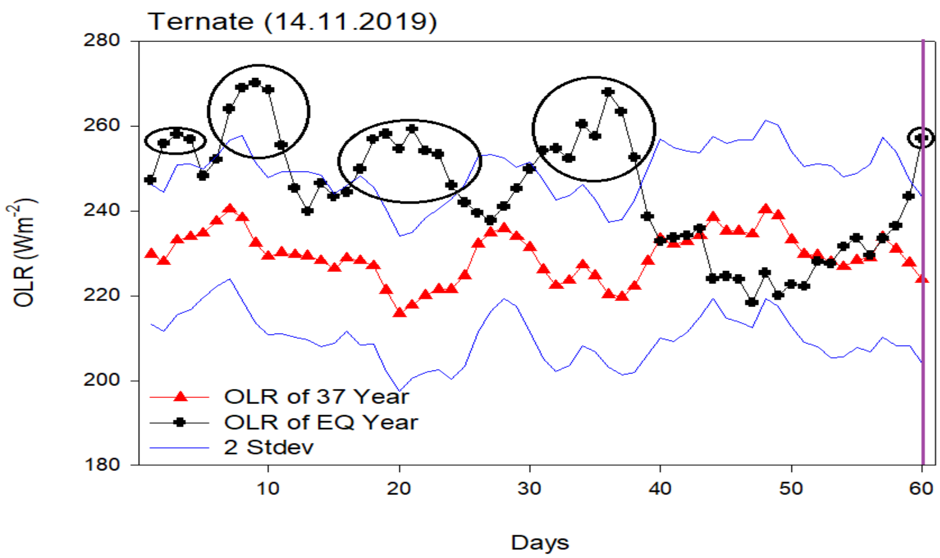

Figure 8. Daily variation of outgoing longwave radiation during the earthquake year (black cross) - 2019 vs. mean historical time series 1982-2018 (red triangle) during the earthquake events that occurred in Ternate, Indonesia on 14.11.2019 having epicentre 1.53° N, 126.41° E. Blue coloured curve indicates 2.0 standard deviation from the mean - historical time series. The purple line shows earthquake day.

8. Ternate (Indonesia)

On November 14, 2019, a magnitude 6.0 (epicentre 1.53° N, 126.41° E) earthquake occurred in Ternate, Indonesia, at a focal depth of 23 km. (Figure 8) shows the comparison between the time series 2019 (earthquake year) with the historical years 1982-2018 time series. The black line with a cross and the red line with a triangle denote the earthquake year and a historical time series of 37 years, respectively. The figure shows that OLR is greater than 2σ on the 2nd to 4th, 7th to 11th, 17th to 24th, 31st to 38th, and 60th day, with the average OLR values during the earthquake year and historical time series being ~256.87 Wm^{-2}, ~265.36 Wm^{-2}, ~254.59 Wm^{-2}, ~257.83 Wm^{-2}, ~257.22 Wm^{-2}, and ~231.66 Wm^{-2}, ~234.07 Wm^{-2}, ~221.62 Wm^{-2}, ~223.25 Wm^{-2}, ~223.94 Wm^{-2} respectively.

9. Bengkulu (Indonesia)

The earthquake that occurred on August 13, 2017, had a magnitude of 6.4 and a focal depth of 31.0 km (epicentre 3.76° S and 101.62° E) in Bengkulu, Indonesia. The variation in OLR has been analysed for the purpose of identifying precursory signatures during the earthquake event. (Figure 9) shows a comparison of the time series year 2017 (earthquake year) with the historical time series years 1980–2016 of OLR. From this figure, one can observe many instances where the OLR is higher than the historical time series. There is an increase in the OLR on the 4th, 9th to 10th, 12th to 13th, 15th and 23rd, days with values ~204.82 Wm^{-2}, ~209.66 Wm^{-2}, ~200.23 Wm^{-2}, ~212.82 Wm^{-2}, and ~212.97 Wm^{-2}, respectively, of greater than 2σ from the mean historical time series. Again, it was found that the OLR values rise from the 28th to 31st days, 38th to 42nd days, and from the 48th to 50th days, with the average OLR values during the earthquake year and historical time series being ~210.04 Wm^{-2}, ~263.61 Wm^{-2}, ~264.99 Wm^{-2}, and ~243.68 Wm^{-2}, ~230.92 Wm^{-2}, ~228.38 Wm^{-2}, respectively. It is clearly observed that the maximum number of anomalies in OLR as precursory signatures are present before the earthquake day.

10. Luwuk (Indonesia)

The next earthquake event occurred on March 15, 2015, with a magnitude of 6.1 (epicentre 0.54° S, 122.30° E) and a focal depth of 31.0 km in Luwuk, Indonesia. (Figure 10) shows a comparison of the time series 2015 (earthquake year) with the historical time series 1978–2014 of OLR. (Figure 10) shows many instances in which the OLR exceeds the 2σ from the mean historical time series. From (Figure 10), one can observe many instances where the OLR is higher than the historical time series. There is an increase in the OLR on the 13th and 53rd, days with values ~232.46 Wm^{-2} and ~247.73 Wm^{-2}, respectively, of greater than 2σ from the mean historical time series. Again, it was found that the OLR values rise from the 36th to 38th days, and from the 47th to 50th days, with the average OLR values during the earthquake year and historical time series being ~171.19 Wm^{-2}, ~182.25 Wm^{-2} and ~217.10 Wm^{-2}, ~228.40 Wm^{-2} respectively. It is observed that the maximum number of anomalies in OLR as precursory signatures are present before the earthquake day.

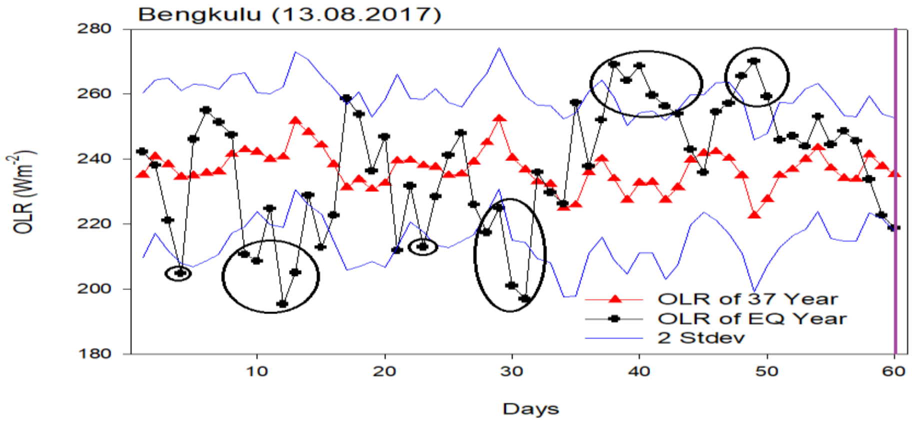

Figure 9. Daily variation of outgoing longwave radiation during the earthquake year (black cross) - 2017 vs. mean historical time series 1980-2016 (red triangle) during the earthquake events that occurred in Bengkulu, Indonesia (13.08.2017) having epicentre 3.76° S, 101.62° E. Coloured curve indicates 2.0 (blue) standard deviation from the mean - historical time series. The purple line shows earthquake day.

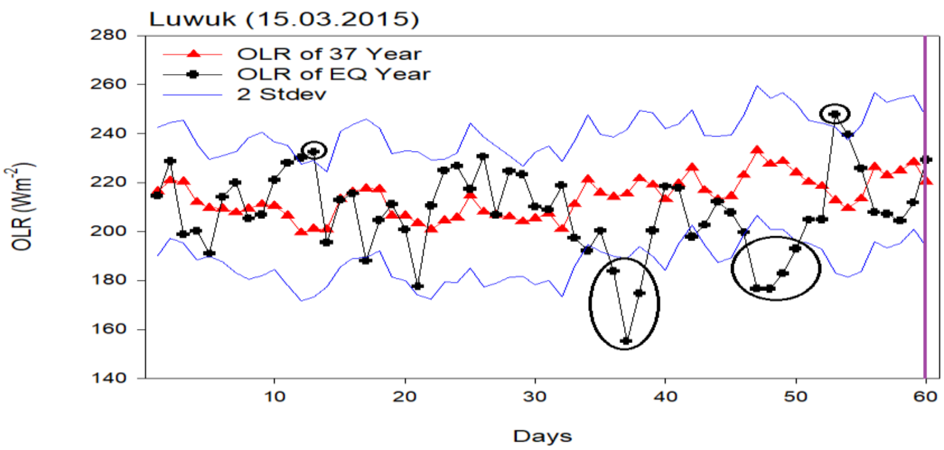

Figure 10. Daily variation of outgoing longwave radiation during the earthquake year (black cross) - 2015 vs. mean historical time series 1978-2014 (red triangle) during the earthquake events that occurred in Luwuk, Indonesia (15.03.2015) having epicentre 0.54° S, 122.30° E. Blue coloured curve indicates 2.0 standard deviation from the mean - historical time series. The purple line shows earthquake day.

Maximum and minimum anomalies in OLR during the earthquake events

One can see from the figures that the OLR exhibited anomalous behaviour during all the earthquake occurrences. The anomaly can be used to identify some of the major warning signs of upcoming earthquakes. Use of the OLR anomaly, will help us better comprehend various earthquake parameters. In the present investigation, we have additionally examined the maximum and minimum OLR anomalies experienced during each earthquake occurrences.

(Table 2A) provides the details of the maximum anomaly in OLR during all the earthquake events. Parameter *D* represents the day when the maximum anomaly in OLR during the EQ year was observed, compared to the historical time series. *X* and *Y* represent the magnitude values of OLR corresponding to that day *(D)* during the EQ year and historical time series respectively. *X/Y* gives the extent of maximum anomaly of OLR during EQ year compared to the historical time series corresponding to day *D*.

The Earthquake that occurred on 10.09.2022 (Pariaman, Indonesia) experienced the highest anomaly on the 6th day before the earthquake day. The corresponding values of OLR during the earthquake year and historical time series were 268.42 Wm^{-2} and 214.54 Wm^{-2} respectively. Thus, the magnitude of the anomaly was registered as 1.25 times greater than the historical series. On 10.09.2022 (Biak, Indonesia) an earthquake occurred with 6.2 magnitude. The highest anomaly was recorded on the 20th day with a magnitude value of OLR 261.17

Table 2A. Details of the maximum observed anomaly in OLR during the earthquake events

Sr. No.	Location	Date and time(UTC)	Epicentre (Lat., Long.)	Maximum anomaly day (D)	Value of OLR during earthquake Year (*X*)	Value of OLR corresponding day of historical time series (*Y*)	*X/Y*
1	Pariaman, Indonesia	10.09.2022 (23:10:43)	1.14° S, 98.65° E	55th	268.42	214.54	1.25
2	Biak, Indonesia	10.09.2022 (00:05:12)	2.23° S, 138.17° E	41st	261.17	215.51	1.21
3	Papua, Indonesia	09.09.2022 (23:31:47)	2.24° S, 138.19° E	40th	261.17	215.51	1.21
4	Pariaman, Indonesia	13.03.2022 (21:09:22)	0.62° S, 98.62° E	58th	251.35	205.69	1.22
5	Gorontalo, Indonesia	06.11.2021 (14:37:36)	0.04° S, 124.28° E	23rd	271.97	234.35	1.16
6	Dhekiajuli, Assam, India	28.04.2021 (02:21:26)	26.78° N, 92.45° E	5th	274.16	220.95	1.24
7	Port Blair, India	17.07.2020 (14:03:40)	11.84° N, 94.93° E	24th	242.89	196.32	1.23
8	Ternate, Indonesia	14.11.2019 (21:12:54)	1.53° N,126.41° E	52nd	270.09	232.33	1.16
9	Bengkulu, Indonesia	13.08.2017 (03:08:10)	3.76° S, 101.62° E	12th	270.16	222.64	1.21
10	Luwuk, Indonesia	15.03.2015 (23:17:16)	0.54° S, 122.30° E	7th	247.73	212.75	1.16

Table 2B. Details of minimum observed anomaly in OLR during the earthquake events

Sr. No.	Location	Date and Time (UTC)	Epicentre (Lat., Long.)	Minimum anomaly day (*D′*)	Value of OLR during earthquake year (*X′*)	Value of OLR corresponding day of historical time series (*Y′*)	*X′/Y′*
1	Pariaman, Indonesia	10.09.2022 (23:10:43)	1.14° S, 98.65° E	49th	159.03	222.57	0.71
2	Biak, Indonesia	10.09.2022 (00:05:12)	2.23° S, 138.17° E	56th	176.40	219.63	0.80
3	Papua, Indonesia	09.09.2022 (23:31:47)	2.24° S, 138.19° E	55th	176.40	219.63	0.80
4	Pariaman, Indonesia	13.03.2022 (21:09:22)	0.62° S, 98.62° E	32nd	163.12	209.98	0.77
5	Gorontalo, Indonesia	06.11.2021 (14:37:36)	0.04° S, 124.28° E	52nd	168.01	253.91	0.66
6	Dhekiajuli,Assam, India	28.04.2021 (02:21:26)	26.78° N, 92.45° E	13th	212.28	233.01	0.91
7	Port Blair, India	17.07.2020 (14:03:40)	11.84° N, 94.93° E	5th	144.72	189.30	0.76
8	Ternate, Indonesia	14.11.2019 (21:12:54)	1.53° N,126.41° E	37th	245.95	221.49	1.11
9	Bengkulu, Indonesia	13.08.2017 (03:08:10)	3.76° S, 101.62° E	49th	195.38	240.74	0.81
10	Luwuk, Indonesia	15.03.2015 (23:17:16)	0.54° S, 122.30° E	24th	155.13	215.43	0.72

Wm^{-2} and 215.51 Wm^{-2} during the earthquake year and historical time series respectively. Thus, a 1.21 times increase in the anomaly was observed. Similarly, all the events in consideration experienced anomalies. The maximum anomaly in OLR was 1.21, 1.22, 1.16, 1.24, 1.23, 1.16, 1.21, 1.16 times greater during the earthquake year compared to the historical time series during 3rd, 4th, 5th, 6th, 7th, 8th, 9th and 10th earthquake events in consideration respectively. The highest anomalies spanned from 1.16 to 1.25 times greater than the historical time series. The details of all the magnitude values of the highest anomaly OLR during EQ year and historical time series events have been summarised in Table 2A.

Similarly, Table 2B provides the details of the minimum anomaly in OLR during all the earthquake events. Parameter D' represents the day when the maximum anomaly in OLR during the earthquake year was observed compared to the historical time series. X' and Y' represent the magnitude values of OLR corresponding to that day *(D')* during the earthquake year and historical time series respectively. X'/Y' gives the extent of the minimum anomaly of OLR during earthquake year compared to the historical time series corresponding to day D'.

The first earthquake event under consideration (10.09.2022; Pariaman, Indonesia) observed the minimum anomaly on the 12th day before the EQ day. During this event, the minimum anomaly observed in OLR during the earthquake year and in the historical time series were 159.03 Wm^{-2} and 222.57 Wm^{-2}, respectively. Thus, resulting in anomalous increase of 0.71 times greater than the historical series. Another earthquake that occurred on September 10, 2022, in Biak, Indonesia, experienced the minimum anomaly in OLR on the 5th day, with values of 176.40 Wm^{-2} during the earthquake year and 219.63 Wm^{-2} in the historical time series respectively. Thus, experiencing an anomalous increase of 0.80 times, compared to historical data. Similar observations were recorded during all the other earthquake events. The minimum anomalous increase in OLR were 0.80, 0.77, 0.66, 0.91, 0.76, 1.11, and 0.81 times greater during the earthquake years, compared to the historical time series during 3rd, 4th, 5th, 6th, 7th, 8th, 9th, and 10th earthquake events in consideration respectively. The minimum anomalies ranged from 0.66 to 1.11 times greater than the values in the historical time series.

(Table 2C and Figure 11) provide a comprehensive overview of the maximum and minimum anomalous increase of OLR during all the EQs. The observed maximum and minimum anomalous increase in OLR spanned from 1.16 to 1.25 and 0.66 to 1.11 times greater during the earthquake years respectively, compared to historical time series during all the ten EQ events. **(**Table 1) lists the locations of all earthquake occurrences. All the earthquakes under consideration had distinctive origins; four of their epicentres were on land, while others were located close to or in the ocean. The OLR anomalies before earthquakes with a magnitude greater than 6.0 that occurred in India and the Indonesian regions have been examined. Outgoing longwave radiation (OLR) refers to infrared radiation continuously emitted from the Earth's surface and subsequently released into the atmosphere. This radiation is measured as the amount of energy emitted per unit area. Before the occurrence of recent highly destructive earthquakes, instances were noted where anomalous positive deviations above the 2σ level were observed two months prior to the earthquake events. For example, Japan (M 9.0, 2011) (Pulinets and Ouzounov, 2011), Sumatra (M 8.2, 2012) (Venkatanathan et al., 2013), and Pakistan (M 7.7, 2013) (Venkatanathan and Natyaganov, 2014) are the cases where strange variation in OLR have been recorded before significant earthquakes. These anomalies appeared at different times and were probably influenced by unusual features of tectonic activity, such as earthquakes, and plate movements, which can significantly influence surface and atmospheric conditions, leading to variations and anomalies in outgoing longwave radiation.

Table 2C. Maximum/minimum anomaly in OLR during all the earthquake events

Sr. No.	Location	Date and time(UTC)	*X/Y*	*X′/Y′*
1	Pariaman, Indonesia	10.09.2022 (23:10:43)	1.25	0.71
2	Biak, Indonesia	10.09.2022 (00:05:12)	1.21	0.80
3	Papua, Indonesia	09.09.2022 (23:31:47)	1.21	0.80
4	Pariaman, Indonesia	13.03.2022 (21:09:22)	1.22	0.77
5	Gorontalo, Indonesia	06.11.2021 (14:37:36)	1.16	0.66
6	Dhekiajuli,Assam,India	28.04.2021 (02:21:26)	1.24	1.11
7	Port Blair, India	17.07.2020 (14:03:40)	1.23	0.76
8	Ternate, Indonesia	14.11.2019 (21:12:54)	1.16	1.11
9	Bengkulu, Indonesia	13.08.2017 (03:08:10)	1.21	0.81
10	Luwuk, Indonesia	15.03.2015 (23:17:16)	1.16	0.72

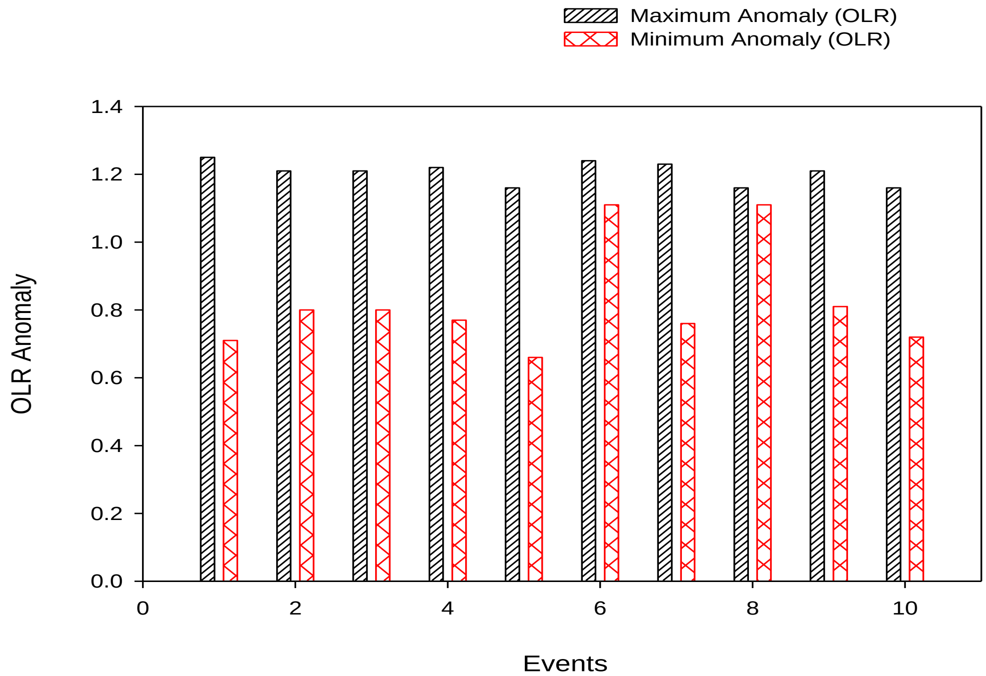

Figure 11. Representation of maximum (black bars) and minimum (red bars) deviation in anomalies of OLR during all the ten earthquake events

DISCUSSION

In the present work, anomalous precursory behaviour of OLR was observed for all the earthquake events. However, they did have distinctive behavioural characteristics. This could be caused by variations in meteorological variables as well as changes in geographic regions. The locations of these ten earthquakes, their epicentres, proximity to the ocean and the robust interplay between land, ocean, and atmosphere, are likely to have a significant impact on the changes in OLR.

All the earthquake events reveal multiple instances where the OLR exceeds the values of the historical time series. Notably, the trends across oceanic and coastal regions are similar. It is observed that the highest number of OLR anomalies, serving as potential precursory signatures, occur several days before the earthquake event. Specifically, a significant increase in OLR is evident between the 30^{th} to 55^{th} days before the all the considered earthquake events, except for Assam, which is a land-based region. The maximum OLR anomaly appears typically around two months before the earthquake, with the earliest anomaly detected as soon as the 5th day (as observed in Assam, India). In Assam, the corresponding OLR values during the earthquake year and the historical time series were 274.16 W/m^2 and 220.95 W/m^2, respectively, indicating that the anomaly was 1.24 times higher than the historical average. Anomalous seismic activity was also observed in Assam for up to two months before the earthquake, likely attributed to the region's high earthquake susceptibility due to its tectonic setting.

The present study's analysis of ten earthquakes over the Indonesian and Indian regions, with magnitudes exceeding 6.0, consistently demonstrated detectable OLR anomalies. These OLR anomalies are likely to be influenced by tectonic activity, plate movements, and related atmospheric and surface conditions that precede the earthquakes. The findings suggest that monitoring OLR variations may offer valuable insights into the development of seismic event and early warning particularly in the regions with oceanic influence.

Prior to an earthquake, the epicentral region experienced an increase in infrared heat (IR), which contributed to severe land-ocean atmospheric interactions and anomalous OLR (Sharma et al., 2024). It is considered that the stress buildup in the epicentral region days before the earthquake served a major role in the increase in infrared temperature immediately preceding the earthquake (Wu and Liu, 2009). Earthquakes can alter the local land surface and atmospheric conditions. For example, the sudden release of energy and the subsequent shifting of the Earth's crust can affect surface temperatures and atmospheric composition, potentially causing anomalies in the measured OLR (Mahmood et al., 2017). Large-scale seismic events can disrupt oceanic and atmospheric patterns. These disruptions can affect sea surface temperatures and atmospheric conditions, leading to anomalies in the OLR detected by satellites (Jiao et al., 2018). The movement of tectonic plates can influence geothermal activity, such as the formation of new geothermal vents. Increased geothermal activity can release additional heat into the atmosphere, affecting local OLR measurements (Rawat et al. 2011). Earthquakes can inject large amounts of ash and gases, such as sulphur dioxide, into the atmosphere. These particles can spread across the globe, reflecting solar radiation and temporarily cooling the Earth's surface. This cooling effect can lead to anomalies in OLR, as the surface emits less infrared radiation due to the lower temperatures. Consequently, monitoring OLR anomalies can help in understanding and potentially predicting the impacts of large-scale seismic events (Xiong and Shen, 2017). Also, the build-up of stress in short focal depth earthquakes is reflected in changes in surface temperature, Surface Latent Heat Flux (SLHF), and Outgoing Longwave Radiation (OLR). As the stress at the fault interface increases, the rocks become compressed, resulting in a reduction in the number of voids within them. The rise and migration of hot radon gases from rock voids toward the Earth's surface , contributes to atmospheric warming (ZiQi et al., 2002). Air ionization also induces thermal effects, such as changes in air humidity and temperature, characterized by an increase in air temperature and a reduction in relative humidity. The rise in surface temperature leads to intensified outgoing thermal radiation, which is particularly noticeable in epicentral regions and corresponds to OLR variations. Continued OLR analysis using various temporally aggregated data (e.g., monthly, daily, from different satellites, and during day/night cycles) holds promise for the early detection of anomalies related to major global earthquakes. However, many theoretical questions remain about the quantitative relationship between longwave radiation flux and seismo-tectonic stress. Despite these uncertainties, OLR could become a valuable parameter in precursor studies, with early anomalies potentially helping to characterize key earthquake parameters, such as location, timing, and magnitude (Pulinets et al., 2006). The appearance of OLR anomalies is influenced by various factors, including earthquake intensity and atmospheric conditions, but is generally correlated with the earthquake's magnitude. All of the occurrences under study have seen the OLR undergo large anomalous changes. Furthermore, anomalies were discovered around 59 days before the earthquake day (i.e. 60^{th} day). Increased tectonic activity in earthquake-prone areas is responsible for these thermal anomalies.

CONCLUSIONS

In this study, we have examined the Outgoing Longwave Radiation (OLR) as a potential precursor to earthquakes, focusing on ten recent high-magnitude ($M \geq 6.0$) seismic events. Our findings lead to the following conclusions:

(i) The OLR values exhibited a consistent anomalous increase during all ten earthquake events analysed in this study.

(ii) In all the earthquake events under consideration, OLR values are found to consistently exhibit anomalous behaviour during the pre-earthquake period, with slight variations in their patterns.

(iii) The maximum observed anomalous increase in OLR ranges from 1.16 to 1.25 times greater during earthquake years when compared to the historical time series across all ten earthquake events.

(iv) The minimum observed anomalous increase in OLR ranges from 0.66 to 1.11 times greater during the earthquake years when compared to the historical time series across all ten earthquake events.

(v) The fluctuations in both the maximum and minimum anomalies of OLR are most pronounced for earthquakes that occurred either directly over the ocean or in proximity to it.

(vi) The behavioural pattern of OLR over the land and ocean/near ocean earthquake events were different owing to diverse crustal properties and atmospheric/ meteorological conditions such as humidity, water vapour content etc.

(vii) The accumulation of water vapour leads to the trapping of outgoing radiation, resulting in elevated temperatures over the EPZ. Consequently, the increase in OLR before all the major earthquake events.

ACKNOWLEDGEMENTS

The authors express their gratitude to the NCEP-NCAR website for providing the Outgoing Longwave Radiation (OLR) data. Additionally, they extend their thanks to the United States Geological Survey (USGS) team for sharing valuable earthquake information.

Author Credit Statement

Problem identification and data analysis were conducted by Pooja Sharma and Ananna Bardhan. All authors collaborated in writing the paper.

Data Availability

The paper provides the data and website information.

Compliance with Ethical standards

The authors declare no conflict of interest and confirm adherence to copyright norms.

References

Akhoondzadeh, M., 2024. Earthquake prediction using satellite data: Advances and ahead challenges. Advances in Space Res., 74 (8), 3539-3555

Bardhan, A., Sharma, P., Sahai, A. and Sharma, D.K., 2022. Ionospheric and surface thermal parameters during three high magnitude earthquakes. J. Ind. Geophys. Union, 26(6), 448-461.

Brohan, P., Kennedy, J.J., Harris, I., Tett, S.F. and Jones, P.D., 2006. Uncertainty estimates in regional and global observed temperature changes: A new data set from 1850. J. Geophys. Res. Atmospheres, 111 (D12). htttps://doi.org/10.1029/2005JD006548

Choudhury, S., Dasgupta, S., Saraf, A.K. and Panda, S., 2006. Remote sensing observations of pre-earthquake thermal anomalies in Iran. Int. J. Remote Sensing, 27(20), 4381-4396. https://doi.org/10.1080/01431160600851827

Dobrovolsky, I.P., Zubkov, S.I. and Miachkin, V.I., 1979. Estimation of the size of earthquake preparation zones. Pure Appl. Geophys., 117(5), 1025-1044.

Fu, C.C., Lee, L.C., Ouzounov, D. and Jan, J.C., 2020. Earth's outgoing longwave radiation variability prior to M≥ 6.0 earthquakes in the Taiwan area during 2009–2019. Frontiers in Earth Sci., 8, 64, p.364.

Ghosh, S., Sasmal, S., Maity, S.K., Potirakis, S.M. and Hayakawa, M., 2024. Thermal Anomalies Observed during the Crete Earthquake on 27 September 2021. Geosciences, 14(3), p.73.

Gruber, A. and Krueger, A., 1984. The status of the NOAA outgoing longwave radiation dataset. Bull. Am. Meteorol. Soc., 65,958–962

Hafeez, A., Ehsan, M., Abbas, A., Shah, M. and Shahzad, R., 2022. Machine learning-based thermal anomalies detection from MODIS LST associated with the M w 7.7 Awaran, Pakistan earthquake. Natural Hazards, 111, 1-19,

Hameed, A., Shah, M., Ghaffar, B., Riaz, S., Jamjareegulgarn, P., Alarifi, N.S. and Abukhadra, M.R., 2024. Possible atmospheric-ionospheric precursors of the 2020 Hotan China earthquake from various satellites. Adv. Space Res., 74(7), 3326-3343.

Jiao, Z.H., Zhao, J. and Shan, X., 2018. Pre-seismic anomalies from optical satellite observations: a review. Natural Hazards and Earth Syst. Sci., 18(4), 1013-1036.

Jing, F., Singh, R.P., Sun, K. and Shen, X., 2018. Passive microwave response associated with two main earthquakes in Tibetan Plateau, China. Adv. Space Res., 62(7), 1675-1689.

Liesmann, B. and Smith, C.A., 1996. Description of a complete (interpolated) outgoing longwave radiation dataset. Bull. Am. Meteorological Soc., 77(6), 1275-1277.

Liu, J.Y., Chuo, Y.J., Shan, S.J., Tsai, Y.B., Chen, Y.I., Pulinets, S.A. and Yu, S.B., 2004, Pre-earthquake ionospheric anomalies registered by continuous GPS TEC measurements. In: Ann. Geophysicae, 22(5), 1585-1593.

Mahmood, I., Iqbal, M.F., Shahzad, M.I. and Qaiser, S., 2017. Investigation of atmospheric anomalies associated with Kashmir and Awaran Earthquakes. J. Atmosph. and Solar-Terrestrial Phys., 154, 75-85.

Niu, F., 2008. Preseismic Velocity Changes Observed from Active Source Monitoring at the Parkfield SAFOD. Info: Lawrence Berkeley National Laboratory.

Ouzounov, D. and Freund, F., 2004. Mid-infrared emission prior to strong earthquakes analyzed by remote sensing data. Adv. space Res., 33(3), 268-273.

Ouzounov, D., Liu, D., Chunli, K., Cervone, G., Kafatos, M. and Taylor, P., 2007. Outgoing long wave radiation variability from IR satellite data prior to major earthquakes. Tectonophysics, 431(1-4), 211-220.

Piscini, A., De Santis, A., Marchetti, D. and Cianchini, G., 2017. A Multi-parametric climatological approach to study the 2016 Amatrice–Norcia (Central Italy) earthquake preparatory phase. Pure Appl. Geophys., 174, 3673-3688.

Piscini, A., Marchetti, D. and De Santis, A., 2019. Multi-parametric climatological analysis associated with global significant volcanic eruptions during 2002–2017. Pure Appl. Geophys., 176, 3629-3647.

Pulinets, S. and Boyarchuk, K., 2004. Ionospheric precursors of earthquakes. Springer Science & Business Media.

Pulinets, S. and Ouzounov, D., 2011. Lithosphere–Atmosphere–Ionosphere Coupling (LAIC) model–An unified concept for earthquake precursors validation. J. Asian Earth Sci., 41(4-5), 371-382.

Pulinets, S.A., Legen'Ka, A.D., Gaivoronskaya, T.V. and Depuev, V.K., 2003. Main phenomenological features of ionospheric precursors of strong earthquakes. J. atmospheric and solar-terrestrial phys., 65(16-18), 1337-1347.

Pulinets, S.A., Ouzounov, D., Karelin, A.V., Boyarchuk, K.A. and Pokhmelnykh, L.A., 2006. The physical nature of thermal anomalies observed before strong earthquakes. Phys. Chem. Earth, Parts A/B/C, 31(4-9), 143-153.

Qasim, M., Shah, M., Shahzad, R. and Jamjareegulgarn, P., 2024. Atmospheric precursors from multiple satellites associated with the 2020 Mw 6.5 Idaho (USA) earthquake. Adv. Space Res., 73(1), 440-455.

Rawat, V., Saraf, A.K., Das, J., Sharma, K. and Shujat, Y., 2011. Anomalous land surface temperature and outgoing long-wave radiation observations prior to earthquakes in India and Romania. Natural hazards, 59, 33-46.

Schulz, J., Meywerk, J., Ewald, S. and Schlüssel, P., 1997. Evaluation of satellite-derived latent heat fluxes. J. Climate, 10(11), 2782-2795.

Shah, M., Tariq, M.A. and Naqvi, N.A., 2019. Atmospheric anomalies associated with Mw> 6.0 earthquakes in Pakistan and Iran during 2010–2017. J. Atmospheric and Solar-Terrestrial Phys., 191, 105056.

Sharma, P., Bardhan, A., Kumari, R., Sharma, D.K., and Sharma, A.K., 2024. Variation of Surface Latent Heat Flux (SLHF) observed during high-magnitude earthquakes. J. Ind. Geophys. Union, 28(2), 131-142.

Tramutoli, V., Cuomo, V., Filizzola, C., Pergola, N. and Pietrapertosa, C., 2005. Assessing the potential of thermal infrared satellite surveys for monitoring seismically active areas: The case of Kocaeli (Izmit) earthquake, August 17, 1999. Remote Sensing of Environment, 96(3-4), 409-426.

Tronin, A.A., 2006. Remote sensing and earthquakes: A review. Phys. Chem. Earth, parts A/B/C, 31(4-9), 138-142.

Tronin, A.A., Hayakawa, M. and Molchanov, O.A., 2002. Thermal IR satellite data application for earthquake research in Japan and China. J. Geodynamics, 33(4-5), 519-534.

Uyeda, S., Nagao, T. and Kamogawa, M., 2009. Short-term earthquake prediction: Current status of seismo-electromagnetics. Tectonophysics, 470(3-4), 205-213.

Venkatanathan, N., Kaarthick, B. and Priyadharshini, C., 2013. OLR anomalies prior to big earthquakes (Mw> 6.0)–a case study on earthquakes of India's neighboring region occurred during the year 2012. New Concepts Global Tecton, 1(3), 34-44.

Venkatanathan, N. and Natyaganov, V., 2014. Outgoing longwave radiations as pre-earthquake signals: preliminary results of 24 September 2013 (M 7.7) earthquake. Curr. Sci., 106(9), 1291-1297.

Weiyu, M., Xuedong, Z., Liu, J., Yao, Q., Zhou, B., Yue, C., Kang, C. and Lu, X., 2018. Influences of multiple layers of air temperature differences on tidal forces and tectonic stress before, during and after the Jiujiang earthquake. Remote sensing of environment, 210, 159-165.

Wu, L. and Liu, S., 2009. Remote sensing rock mechanics and earthquake thermal infrared anomalies. In: Advances in Geoscience and Remote Sensing. Intech Open. DOI:10.5772/8292

Xiong, P. and Shen, X., 2017. Outgoing longwave radiation anomalies analysis associated with different types of seismic activity. Adv. Space Res., 59(5), 1408-1415.

Zhang, W., Zhao, J., Wang, W., Ren, H., Chen, L. and Yan, G., 2013. A preliminary evaluation of surface latent heat flux as an earthquake precursor. Natural Hazards and Earth Sys. Sci., 13(10), 2639-2647.

Ziqi, G., ShuQing, Q., Chao, W., Zhi, L., Xing, G., Weiguo, Z., Yong, Y., Hong, Z. and Jishuang, Q., 2002, The mechanism of earthquake's thermal infrared radiation precursory on remote sensing images. In: IEEE Int. Geosci. Remote Sensing Symp., 4, 2036-2038. IEEE.

Received on: 28-05-2024; Revised on: 14-01-2025; Accepted on: 14-01-2025